COMBINED CONDUCTIVE-RADIATIVE HEAT TRANSFER ANALYSIS IN COMPLEX GEOMETRY USING THE MONTE CARLO METHOD

Cyril Caliot, Stéphane Blanco, Christophe Coustet, Mouna El-Hafi, Vincent Eymet, Vincent Forest, Richard A Fournier, Benjamin Piaud

COMBINED CONDUCTIVE-RADIATIVE HEAT TRANSFER ANALYSIS IN COMPLEX GEOMETRY USING THE MONTE CARLO METHOD

Cyril Caliot[a*], Stéphane Blanco[b], Christophe Coustet[c], Mouna El Hafi[d], Vincent Eymet[c], Vincent Forest[c], Richard Fournier[b], Benjamin Piaud[c]

[a] Processes, Materials and Solar Energy Laboratory, French National Center for Scientific Research, Odeillo, France, cyril.caliot@promes.cnrs.fr
[b] Laboratoire Plasma et Conversion de l'Energie, Paul Sabatier University, Toulouse, France, richard.fournier@laplace.univ-tlse.fr.
[c] MESO-STAR SAS, Longages, France, www.meso-star.com
[d] RAPSODEE, UMR CNRS 5302, MINES-ALBI Université Fédérale de Toulouse, Albi, France, elhafi@mines-albi.fr.

ABSTRACT. Deterministic methods are commonly used to solve the heat balance equation in three-dimensional (3D) geometries. This article presents a preliminary study to the use of a stochastic method for the computation of the temperature in complex 3D geometries where the combined conductive and radiative heat transfers are coupled in the porous solid phase. The Monte Carlo algorithm and its results are validated by a comparison with the results obtained with a conventional finite-volume method.

INTRODUCTION

Solving combined heat transfers usually requires deterministic methods to solve heat balance equations computing the temperature fields in each phase of the geometry at hand. The most frequently used methods are the finite element and finite volume methods which are widely implemented in commercial software. For combined conductive-radiative heat transfer problems, several deterministic methods were used: (1) Finite volume [1]; (2) Finite element [2]; (3) Lattice Boltzmann [3]. Recently, a stochastic method, based on an Ito-Taylor algorithm (random walk in the solid), was developed for the calculation of the effective conductivity (conduction-radiation) in a representative elementary volume (VER) considering a detailed 3D geometry (Solid phase opaque-vacuum). This method uses the statistics of the positions of the walkers at the stationary regime or the distribution of temperature for the calculation of the effective conductivity [4]. Another stochastic method was presented [5] that implements an integral formulation of the temperature in the case of combined conductive-convective-radiative transient heat transfers. This method allows one, under some conditions [5] insuring a linear relationship with the temperature (including the radiative term linearization, the independence of properties with the temperature and the uniform fluid temperature), to transform the heat balance equation in each media in a Fredholm integral equation of the second kind. It is then possible to write an integral formulation of the Fredholm equation [6] and to use a stochastic resolution technique with the Monte Carlo method with null-collision [7] (it's a meshless method but still requires the spatial distribution of thermophysical and intrinsic radiative properties) enabling efficient numerical tools from computer graphics 3D rendering to be implemented to solve the radiative heat transfer in complex 3D geometries. The use of a Monte Carlo method (delivering a result with a confidence interval) and efficient numerical tools for the computation of a local temperature, while accounting for the combined heat transfers (even linearized), allows one to get reference solutions (if linearization assumptions are verified) to validate other methods when they are implemented in complex geometries. The article follows this approach of inter-comparison between the stochastic method and a deterministic method in order to calculate the temperature of the solid in a porous medium consisting of a transparent phase (void) and an opaque solid phase possessing a complex architectural geometry (3D). Thanks to the integral formulation, the method presented makes it

possible to evaluate the temperature at a point, the paths all starting from this point (inverse formulation). If necessary, an additional random sampling enables to calculate averages on surfaces or volumes. In [4], on the contrary, the formulation is direct and the walkers, initially distributed over the whole domain, are used to evaluate mean temperatures or fluxes. Indeed, in these direct particle methods, there is an important dependence of computational performances on the complexity of the geometry (which disappears completely in a backward formulation of the problem, except for the evaluation of the field). On the other hand, the method in [4] benefits from the same advantages as those of the backward formulation when walkers are starting from a VER to evaluate the effective conductivity.

The objective of this communication is to present and discuss the comparison between the results obtained with the stochastic method and the finite volume method in a 3D complex geometry where the stationary conductive and radiative heat transfers are combined. The section 2 presents the stochastic method, the section 3 describes the deterministic method and within the section 4, a comparison between the two methods is discussed.

STOCHASTIC METHOD

The method presented in [5] is here simplified (stationarity, opaque solid, no convection) and the resulting algorithm will be comprehensively described. The heat balance equation in a homogeneous solid at the stationary regime, without any heat volumetric sources, has the following expression in an orthonormal basis:

$$\frac{\partial^2 T}{\partial x^2}+\frac{\partial^2 T}{\partial y^2}+\frac{\partial^2 T}{\partial z^2}=0 \qquad (1)$$

A Monte Carlo method called the “spherical process” or “floating random walk” is used to solve the boundary value problem of the Laplace’s equation (1) in the solid. Haji-Sheikh and Sparrow applied this method in heat transfer problems [8]. This method starts by drawing a sphere included in the solid region and centered at the point the temperature is needed. The radius is usually chosen to draw the largest sphere inscribed and with one point tangent to the boundary. This ensures the random walk to not cross the boundary but require defining a thickened boundary. However, the radius of the sphere is chosen constant in this study with value δ_{diff}. The implemented recursive algorithm for the random walk inside the solid is depicted in Fig. 1 and detailed in Fig. 2. It consists in drawing a sphere of radius δ_{diff}, centered at $\boldsymbol{x_0}$, and in sampling uniformly a point on the sphere surface. If this point $\boldsymbol{x_1}$ is inside the solid, the temperature not known and the spherical sampling continues. By repeating this algorithm a 3D diffusion path is established and visits the solid interior until reaching the boundary ($\boldsymbol{x_b}$, solid-vacuum interface). The temperature value $T(\boldsymbol{x})$ initially sought will ultimately be the temperature value at the wall (boundary). If this temperature is known, the algorithm stops. If not, the balance of the conductive and radiative fluxes (convection is not present, vacuum) at the wall interface is used:

$$-\boldsymbol{n}\cdot\lambda\boldsymbol{\nabla}T=\int_{2\pi}|\boldsymbol{v}\cdot\boldsymbol{n}|\,\epsilon(\boldsymbol{x_b},\boldsymbol{v})[I_b(\boldsymbol{x_b})-I(\boldsymbol{x_b},-\boldsymbol{v})]d\omega(\boldsymbol{v}) \qquad (4)$$

For the sake of clarity, total radiative quantities (average on the entire spectrum) are considered in this article. Because the temperature is unknown and the dependency of the Blackbody intensity (I_b) with the temperature is non-linear, to keep on using the standard Monte Carlo algorithm (linear) the Blackbody intensity should be linearized around a reference temperature (T_{ref}) :

$$I_b(\boldsymbol{x})=\frac{\sigma}{\pi}T^4(\boldsymbol{x})\approx\frac{\sigma}{\pi}T_{ref}^4+4\frac{\sigma}{\pi}T_{ref}^3\big(T(\boldsymbol{x})-T_{ref}\big) \qquad (5)$$

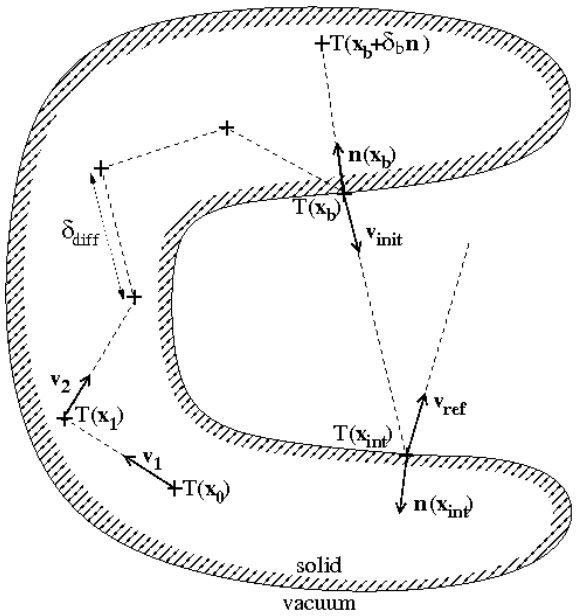

Figure 1. Schematic of possible diffusion and ray paths implemented in the Monte Carlo algorithm

Check input position $\mathbf{x_0}$ belongs to a solid
Choice of spatial step δ_{diff} (arbitrary)
Uniform sampling of a direction $\mathbf{v}$ over 4π sr
Evaluation of position $\mathbf{x_1} = \mathbf{x_0} + \delta_{diff}\mathbf{v}$
if $\mathbf{x_1}$ *belongs to a solid* **then**
  $T(\mathbf{x_0}) = T(\mathbf{x_1})$ (recursive call)
else
  Identification of position $\mathbf{x_b}$, intersection between $\mathbf{x_1}$-$\mathbf{x_0}$ and the boundary of the solid
  $T(\mathbf{x_0}) = T(\mathbf{x_b})$
end

Figure 2. Algorithm to evaluate $\mathbf{T(x_0)}$ in the solid

Check input position $\mathbf{x_b}$ is on a solid boundary
Choice of spatial step δ_b (arbitrary)
Uniform sampling of a random number r over [0,1]
if $r < \frac{\lambda/\delta_b}{\left(\lambda/\delta_b + h_r(\mathbf{x_b})\right)}$ **then**
  $T(\mathbf{x_b}) = T(\mathbf{x_b} - \delta_b\,\mathbf{n})$ (temperature in the solid)
else
  $T(\mathbf{x_b}) = T_{rad}(\mathbf{x_b})$ (radiative temperature)
end

Figure 3. Algorithm to evaluate $\mathbf{T(x_b)}$ at the solid-vacuum interface for total radiative quantities

In addition, the incident radiative intensity ($I(\boldsymbol{x_b}, -\boldsymbol{v})$) depends on the temperature field and the wall reflectivity of the geometry. This term is thus developed with the introduction of the BRDF (Bidirectional Reflectance Distribution Function, product of a density probability over the reflected directions, p_P, and the directional-hemispherical reflectivity, $\rho'^{\cap}$) :

$$I(\boldsymbol{x_b}, -\boldsymbol{v_{init}}) = I(\boldsymbol{x_{int}}, -\boldsymbol{v_{init}}) = \epsilon(\boldsymbol{x_{int}}, -\boldsymbol{v_{init}}) I_b(\boldsymbol{x_{int}}) + \int_{2\pi} p_P(\boldsymbol{x_{int}}) \rho'^{\cap} |\boldsymbol{v}\cdot\boldsymbol{n}|\, I\left(\boldsymbol{x_{int}}, -\boldsymbol{v_{ref}}\right) d\omega(\boldsymbol{v}) \qquad (6)$$

Equation 6 expresses the incident radiative intensity is equal to the intensity leaving from $\boldsymbol{x_{int}}$ because the separating medium is non-participating and transparent (vacuum). This radiative intensity contains a directional contribution associated to the emission and the reflection which is integrated over the incident directions. In the integral over the incident directions of (6), incident radiative intensities are included and they can be expressed also by (6) with some proper changes of the position and direction dependencies. Thus, nested integrals appear that are the basis for an iterative algorithm given in Fig. 3. To alleviate notations, these nested multiple integrals are represented by the notation of (7) highlighting the multiple reflection optical path, noted γ, which belongs to the space of optical paths Γ, started at $\boldsymbol{x_b}$.

$$I(\boldsymbol{x_b}, -\boldsymbol{v_{init}}) = \int_{\Gamma} p_{\Gamma} I_b\left(\boldsymbol{x_\gamma}\right) d\gamma \qquad (7)$$

By introducing an infinitesimal length, δ_b, the temperature gradient at the wall (4) in the solid side, may be discretized as:

$$-\boldsymbol{n}\cdot\lambda\boldsymbol{\nabla}T \approx -\frac{\lambda}{\delta_b}[T(\boldsymbol{x_b}) - T(\boldsymbol{x_b}-\delta_b\boldsymbol{n})] \tag{8}$$

Moreover, the Blackbody intensity in the second term of (4) leads to rewrite this second term (by replacing the directional emissivity by a probability density on the emission direction p_E, and the hemispherical emissivity, ϵ_h) :

$$\int_{2\pi}|\boldsymbol{v}\cdot\boldsymbol{n}|\,p_E\,\epsilon_h[I_b(\boldsymbol{x_b}) - I(\boldsymbol{x_b},-\boldsymbol{v})]d\omega(\boldsymbol{v}) \approx$$
$$h_r T(\boldsymbol{x_b}) - h_r\int_{2\pi}\frac{|\boldsymbol{v}\cdot\boldsymbol{n}|}{\boldsymbol{\pi}}\,p_E\int_{\Gamma}\,p_\Gamma T(\boldsymbol{x_\gamma})\,d\gamma\,d\omega(\boldsymbol{v}) \tag{9}$$

with $h_r = 4\epsilon_h\sigma T_{ref}^3$ the linearized radiative exchange coefficient. The nested integrals of the second term represents an average temperature, noted T_{rad}, seen by radiation at $\boldsymbol{x_b}$. Indeed, $\left(\frac{|\boldsymbol{v}\cdot\boldsymbol{n}|}{\boldsymbol{\pi}}p_E\right)$ represents a probability density function for the choice of the solid angle, $\omega(\boldsymbol{v})$, and p_Γ is the density probability associated to optical path constituted of multiple reflections.

Sampling of a emission direction $\mathbf{v_{init}}$ according to $\frac{|\mathbf{v_{init}}\cdot\mathbf{n}(\mathbf{x_b})|}{\pi}p_\epsilon(\mathbf{v_{init}})$
Generation of the optical path initiated at $\mathbf{x_b}$, in direction $\mathbf{v_{init}}$
Identification of the first intersection $\mathbf{x_{int}}$ between the optical path and the boundary of the solid
Uniform sampling of a random number r over $[0,1]$
if $r < \epsilon_h$ **then**
  $T_{rad}(\mathbf{x_b}) = T(\mathbf{x_{int}})$ (boundary temperature)
else
  sampling of a reflexion direction $\mathbf{v_{ref}}$ according to $\frac{|\mathbf{v_{ref}}\cdot\mathbf{n}(\mathbf{x_{int}})|}{\pi}p_\epsilon(\mathbf{v_{ref}})$
  $T_{rad}(\mathbf{x_b}) = T_{rad}(\mathbf{x_{int}})$ (recursive call)
end

Figure 4. Algorithm to evaluate $\mathrm{T_{rad}}(\mathbf{x_b})$ at the solid-vacuum interface for total radiative quantities

By combining (8) and (9), an expression of the temperature at $\boldsymbol{x_b}$ may be obtained:

$$T(\boldsymbol{x_b}) = \frac{\lambda/\delta_b}{\frac{\lambda}{\delta_b}+h_r}T(\boldsymbol{x_b}-\delta_b\boldsymbol{n}) + \frac{h_r}{\frac{\lambda}{\delta_b}+h_r}T_{rad}(\boldsymbol{x_b}) \tag{10}$$

Equation (10) highlights two weights (or probability) multiplied by temperatures that are representatives of the conduction and radiation heat transfers. The more h_r is important compared with $\frac{\lambda}{\delta_b}$, the more the algorithm chooses to compute T_{rad} instead of $T(\boldsymbol{x_b}-\delta_b\boldsymbol{n})$. In addition to the representation of the physics brought by (10), the statistics of the generated paths may contain information allowing a better understanding of the major heat transfer mechanisms. The algorithm requires choosing arbitrarily the values of δ_{diff} and δ_b. For the transient regime, the value of δ_{diff} should be very small compared to the characteristic length of the solid to accurately solve (1). But for the stationary regime assumed in this study, because the local temperature at $\boldsymbol{x_0}$ is equal to the average temperature on a sphere centered at $\boldsymbol{x_0}$ with an arbitrary radius (provided the sphere is included in the solid), the value of δ_{diff} may be as high as needed to reduce the computation time. However, δ_b should be small enough for (8) to be valid. Moreover, when $T(\boldsymbol{x_b}-\delta_b\boldsymbol{n})$ is evaluated the algorithm in Fig. 2 is used and the condition of its validity is thus given by $\delta_b > \delta_{diff}$ which ensures to sample the complete sphere surface having a radius δ_{diff} and included within the solid. Many options exist to set those values, but in this study constant values were set smaller than the minimum length existing inside the solid.

This stochastic method allows one to compute the temperature at one position inside the solid ($T(\boldsymbol{x})$) using a Monte-Carlo algorithm to solve a conductive-radiative heat transfer problem (solid-vacuum media) thanks to the linearization assumption of the Blackbody intensity and the independence of the solid conductivity and radiative properties with temperature. It is therefore possible to compute any linear integral of the temperature such as an integral of the solid temperature on a cutting plane (S) which intersects the solid:

$$\langle T \rangle = \int_S \; p_S \, T(\boldsymbol{x}) d\boldsymbol{x} \tag{11}$$

With ($p_S = \frac{1}{S}$) the uniform probability density function leading to uniformly sample the positions $\boldsymbol{x}$ in S which belongs to the solid and where the temperature is computed.

DETERMINISTIC METHOD

The finite volume method [9] implemented in the commercial software ANSYS Fluent is described in details in their documentation [10]. The balance energy equation inside the solid and the radiative transfer equation are solved at the stationary regime. However, a fluid zone must be defined with a mesh to enable the resolution of the radiative transfer (with the Discrete Ordinates method) combined to conduction in the solid. This fluid zone has a zero absolute pressure (vacuum) and the fluid dynamics are not solved. The spatial discretization schemes use a least-square-fitting method to evaluate the gradients, a second-order Upwind method for the energy balance and a first-order Upwind method for the Discrete Ordinates (with 6*6 discretizations per octant, and a pixelation of 6*6). In addition to the wall temperature boundary conditions where they are defined, the interfaces between the fluid and the solid are coupled, allowing the continuity of the radiative flux in the vacuum with the conductive flux in the solid.

RESULTS AND DISCUSSION

The objective of the simulations is to solve the solid temperature average in the XZ-plane of a complex geometry depicted in Fig. 5. The conduction-radiation problem is considered at the stationary regime, the solid is opaque and there is no convection. The geometry represents a porous medium (stacked Kelvin's cells) between two walls with their end faces maintained at a fixed temperature ensuring a thermal gradient in the medium. A symmetry condition is applied for the four lateral faces. The porous medium thickness (along the Y-axis) is 12 mm corresponding to 3 Kelvin's cells (d_c=4 mm, cell diameter) and the thickness of a plate is 2 mm. The strut diameter is about d_s=0.5 mm. The contact resistances between the porous medium and the plates are neglected. The medium is infinite in the X and Z directions. In a first case, the temperatures are set to 300 and 310 K, $T_{ref} = 305$ K, and two thermal conductivity (low and high) values are considered. In a second case, higher temperatures are chosen, 1000 and 1500 K, $T_{ref} = 1250$ K, and two thermal conductivity are also considered to lead to a diffusion probability given in (10), $p_{diff} = \left(\frac{\lambda}{\delta_b}\right) / \left(\frac{\lambda}{\delta_b} + h_r\right)$, of 0.1 and 0.9 (see Table 1). For all the cases, the solid emissivity is assumed gray (ϵ_h =0.85) and diffuse. For the stochastic method, the arbitrary diffusions steps are chosen: $\delta_b = 0.1$ mm et $\delta_{diff} = \frac{\delta_b}{2}$. Sixty-four parallel planes to the XZ-plane are retained to compute the average solid temperature (the step is thus 0.25 mm). For each plane, 10^5 Monte-Carlo realizations are used. The Monte-Carlo results are plot with error bars representing a confidence interval of 99.7 %. For the deterministic method, forty-one planes are retained to compute the average solid temperature (comprising planes with a step of 0.5 mm, and eight more are added around the interface between the plate and the porous). The results in terms of average temperatures are presented in Figs 6 and 7 (for the two values of thermal conductivity). These results were obtained by neglecting or accounting for the radiative transfers to identify their effects on the comparison of the two methods.

Table 1: Cases considered in the comparison between the methods ($\delta_b = 0.1$ mm)

Case	λ (W.m^{-1}.K^{-1})	p_{diff}	T_{min} -T_{max} (K)
1a	40	0.999	300-310
1b	10^{-3}	0.65	300-310
2a	4.2 10^{-3}	0.1	1000-1500
2b	3.765 10^{-2}	0.9	1000-1500
3	40	0.999	1000-1500

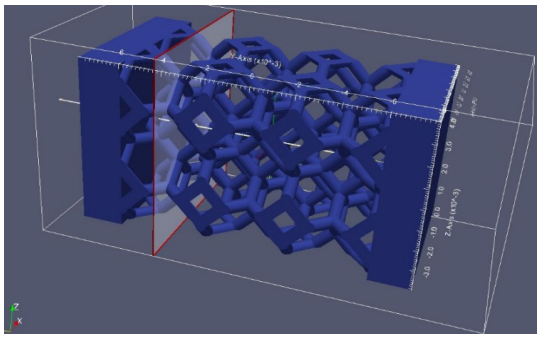

Figure 5. Schematic of a portion of the studied complex 3D geometry (Kelvin cells between two infinite plates) and XZ plane used to average the solid temperatures

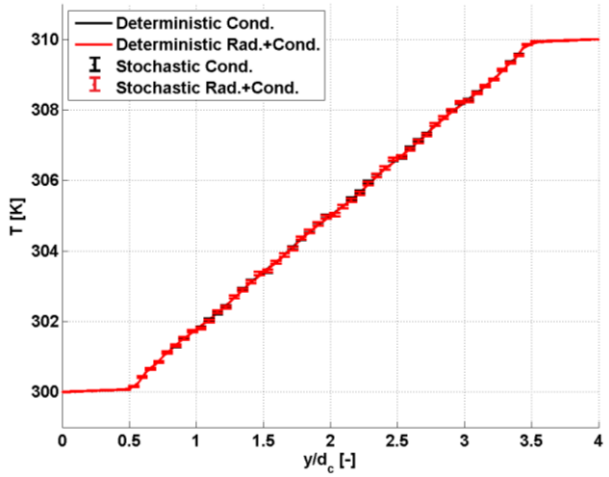

Figure 6. Profiles of the average solid temperatures (case 1a, Table 1) with respect to the non-dimensional thickness

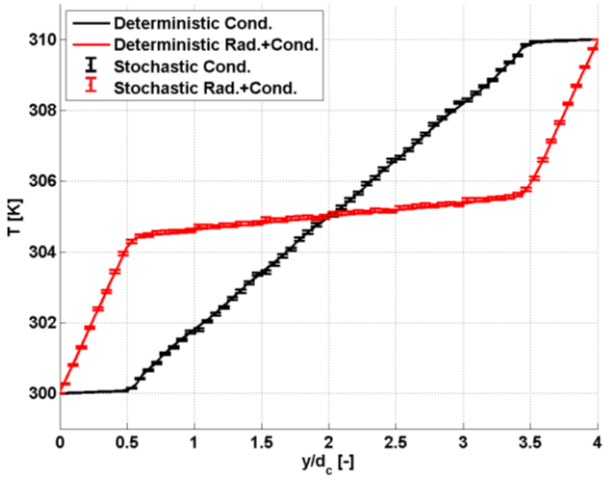

Figure 7. Profiles of the average solid temperatures (case 1b, Table 1) with respect to the non-dimensional thickness

Fig. 6 shows the simulation results obtained with ANSYS Fluent (Deterministic) are confounded when the radiation is neglected (Cond.: pure conduction) and when radiation is accounted for (Rad.+Cond.: radiation combined to conduction). Indeed, the role of radiation is negligible compared to the conduction because the linearized radiative exchange coefficient is negligible compared to the one for conduction: $h_r \cong 5.5$ W.m^{-2}.K^{-1} and $\frac{\lambda}{\delta_b} = 4.10^5$ W.m^{-2}.K^{-1}. When conduction dominates, the stochastic method gives the same results than the deterministic method. The maximum discrepancies between both methods are lower than 0.05K.

For the results in Fig. 7, the thermal conductivity being much lower, the exchange coefficients are of the same order of magnitude: $\frac{\lambda}{\delta_b} = 10$ W.m^{-2}.K^{-1}. For pure conduction in Fig. 7, the same results as in Fig. 6 were obtained because (1) is solved and it does not depend on the thermal conductivity. In the coupled case (Fig. 7), the influence of radiation is highlighted: it increases the flux crossing the medium and homogenizes the temperature of the porous medium. Maximum discrepancies are found lower than 0.1 K.

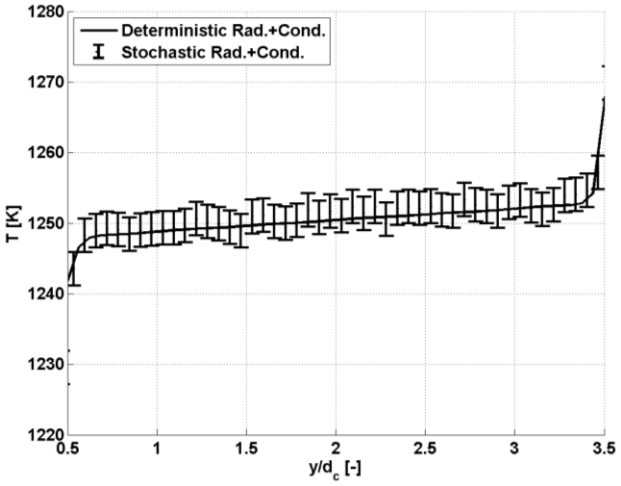

Figure 8. Profiles of the average solid temperatures (case 2a, Table 1) inside the porous medium with respect to the non-dimensional thickness

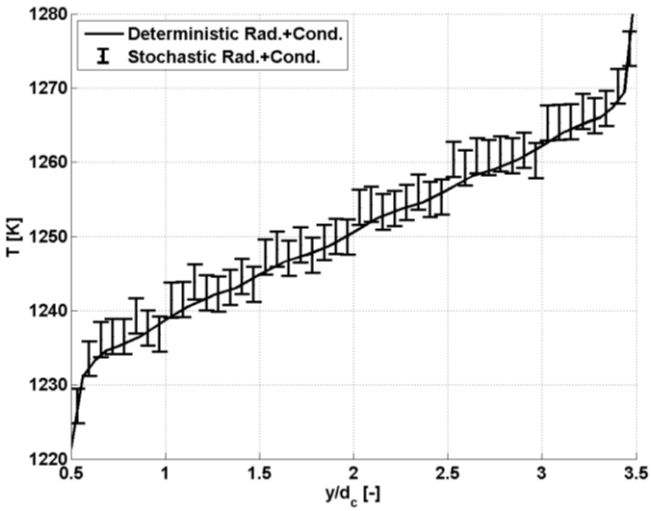

Figure 9. Profiles of the average solid temperatures (case 2b, Table 1) inside the porous medium with respect to the non-dimensional thickness

Figures 8 and 9 present the profiles of the average temperature along the XZ-plane for the end plates at high temperature. When radiation (Fig. 8) or conduction (Fig. 9) dominates in (10) (see case 2a and 2b in Table 1), the stochastic method gives similar results compared to the deterministic method with a 99.7 % confidence interval of less than +/- 2.5 K.

To deepen the comparison, the computation time required by each method to produce the temperature profiles of case 3 is given in Table 2. Several values of δ_b were used and temperature discrepancies associated to these values are shown in Figure 10. The computation time of the cases 1 and 2 are not given here but for the deterministic method it was found to drastically increase with the influence of radiation while it was found similar for the probabilistic method.

Table 2: Computation times required to obtain the temperature profiles using the stochastic method for case 3 (Table 1) depending on δ_b values and compared to the deterministic method

δ_b (m)	CPU Time for 64 Monte Carlo runs (s)	CPU Time for 700 iterations of FLUENT (s)
10^{-4}	616922	151200
$2\ 10^{-4}$	158745	
$3\ 10^{-4}$	73679	
$5\ 10^{-4}$	29994	

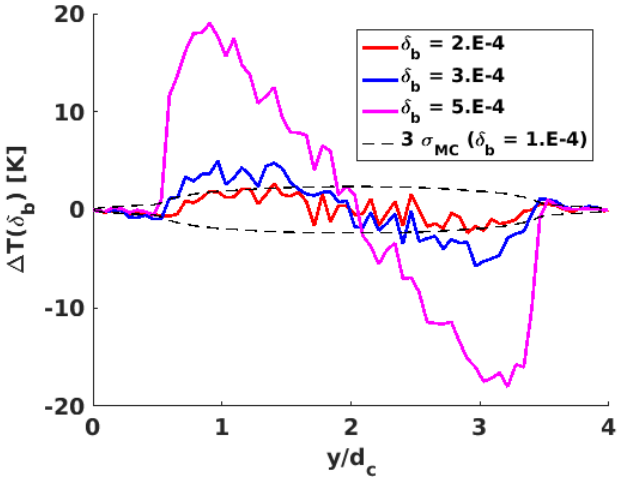

Figure 10. Temperature difference along the geometry thickness (reference results are obtained with δ_b=10^{-4} *m*)

As the value of δ_b increases the MC computation time decreases but the error on the temperature profile increases (see Figure 10). If the entire temperature field is sought the deterministic method is preferable but if the objective of the computation is to found a local temperature and if the space of variables is larger (*e.g.*, adding a wavelength integration) the stochastic method becomes competitive.

CONCLUSION

A Monte Carlo algorithm was established to solve the combined conduction and radiation heat transfers in complex geometries and at the stationary regime. The originality of the approach is to extend the spherical process method for the Dirichlet problem of the Laplace's equation in a solid region to the combined conductive and radiative heat transfer in non-convex geometry with opaque solid and vacuum regions. The steps and assumptions of the model were detailed, especially the need on the integral linearity toward the solid temperature. An implementation in complex geometry was presented and the results were compared to those obtained with the widely used finite volume method (ANSYS Fluent software). When conduction or radiation dominates the heat transfers, the stochastic method reproduces well the results of the finite volume method and it is considered numerically validated. The extension of this probabilistic method to solid materials with any angular and spectral dependency is straightforward. Future work could be related to heterogeneous materials and non-linear heat transfer (temperature dependence of the conductivity and non-linear radiative transfer).

ACKNOWLEDGMENTS

This work was supported by the project OPTISOL (ANR-11-SEED-009) and by the French « Investments for the future » program (contracts ANR-10-LABX-22-01-SOLSTICE and ANR-10-EQPX-49-SOCRATE) both managed by the National Agency for Research.

REFERENCES

1. Y. Sun, X. Zhang, J.R. Howell, Evaluation of three different radiative transfer equation solvers for combined conduction and radiation heat transfer, J Quant Spectr Rad Transfer 2016; 184:262-273.
2. D. Hardy, Y. Favennec, G. Domingues, B. Rousseau, 3D Radiative Transfer Equation Coupled with Heat Conduction Equation with Realistic Boundary Conditions Applied on Complex Geometries, J of Applied Mathematics and Physics 2016;4:1488-1493.
3. S.C. Mishra, H.K. Roy, Solving transient conduction–radiation problems using the Lattice Boltzmann method and the finite volume method, J Comput Phys 2007 ;233: 89-107.
4. G. L. Vignoles, A hybrid random walk method for the simulation of coupled conduction and linearized radiation transfer at local scale in porous media with opaque solid phases, Int. J. of Heat and Mass Transfer 2016;93:707-719.
5. R. Fournier, S. Blanco, V. Eymet, M. El Hafi, C. Spiesser. Radiative, Conductive and Convective Heat-Transfers in a Single Monte Carlo Algorithm, Journal of Physics: Conference Series 2016;676:012007.
6. J. Delatorre, G. Baud, J.-J. Bezian, S. Blanco, C. Caliot, J.-F. Cornet, C. Coustet, J. Dauchet, M. El Hafi, V. Eymet, R. Fournier, J. Gautrais, O. Gourmel, D. Joseph, N. Meilhac, A. Pajot, M. Paulin, P. Perez, B. Piaud, M. Roger, J.-Y. Rolland, F. Veynandt, S. Weitz, Monte Carlo advances and concentrated solar applications, Solar Energy 2014;103:653-681.
7. M. Galtier, S. Blanco, C. Caliot, C. Coustet, J. Dauchet, M. El Hafi, V. Eymet, R. Fournier, J. Gautrais, A. Khuong, B. Piaud, G. Terree, Integral formulation of null-collision Monte Carlo algorithms, J. Quant. Spectr. Rad. Transfer 2013;125:57-68.
8. A. Haji-Sheikh, E. M. Sparrow, The floating random walk and its application to Monte Carlo solutions of heat equations, J. SIAM Appl. Math. 1966;14(2);370-389.
9. S. V. Patankar, Numerical heat transfer and fluid flow, Hemisphere Publish Corp; 1980.
10. ANSYS Inc. PDF Documentation for Release 15.0 ES – Available at: http://148.204.81.206/Ansys/readme.html [accessed 31.01.2017].